Energy 119 (2017) 138–151

Contents lists available at ScienceDirect

Energy

journal homepage: www.elsevier.com/locate/energy

Spray characteristics, engine performance and emissions analysis for Karanja biodiesel and its blends

Sanghoon Lee [a], Chang Sik Lee [b], Sungwook Park [b, *], Jai Gopal Gupta [c, 1], Rakesh Kumar Maurya [c, 2], Avinash Kumar Agarwal [c]

[a] Graduate School of Hanyang University, Seoul, 04763, Republic of Korea
[b] School of Mechanical Engineering, Hanyang University, Seoul, 04763, Republic of Korea
[c] Department of Mechanical Engineering, Indian Institute of Technology Kanpur, Kanpur, 208016, India

ARTICLE INFO

Article history:
Received 29 May 2015
Received in revised form
26 November 2016
Accepted 11 December 2016

Keywords:
Karanja oil methyl ester
Injection rate
Spray visualization
Brake specific fuel consumption
Particulate number concentration
Particulate size distribution

ABSTRACT

The purpose of this paper is to investigate the effects of blending ratio of Karanja oil methyl ester (KOME) on spray characteristics and to analyze the engine performance and exhaust emissions of Karanja biodiesel blend vis-a-vis baseline diesel. Spray characteristics were analyzed using injection rate and spray visualization experiments for the following injection pressures: 50, 100 and 150 MPa. Engine performance, emission and combustion characteristics were also investigated at various engine operation conditions.

From a comparison of the spray evolution of Karanja biodiesel 40% (v/v) blend (KB40) vis-a-vis baseline diesel, the spray shape revealed a narrower and deeper penetrating spray development process for KB40. However, at an ambient pressure of 4 MPa, which is considered to be similar to the cylinder pressure of a test engine, KB40 exhibited a spray evolution behavior (spray penetration and shape) closely resembling that of diesel. In the engine experiment, lower max torque, brake thermal efficiency (BTE) and exhaust gas temperature, in addition to higher brake-specific fuel consumption (BSFC) were observed for biodiesel blend compared to diesel due to lower heating value of Karanja biodiesel.

1. Introduction

In the interest of increasing diversity of energy sources and to reduce the galloping petroleum consumption, the possibility of using alternative fuels for internal combustion engines are being explored worldwide. Amongst various alternative fuels, biodiesel has emerged as a promising substitute for the compressed ignition (CI) engines due its similar properties as that of petroleum diesel and its environmental benefits [1]. Biodiesel can be produced from edible or non-edible vegetable oils and is regarded as renewable, biodegradable and non-toxic fuel [1,2]. In addition, biodiesel contains oxygen, therefore it reduces harmful engine-out emissions and improves engine combustion performance [3,4]. For these reasons, biodiesel is considered as a promising fuel for Internal Combustion (IC) engines, and is widely used either as pure fuel or blended with mineral diesel in varying proportions, depending on availability.

Significant number of research studies have been carried out for successful usage of biodiesel in IC engine and these studies have reported on various aspects of spray characteristics, engine performance, emission characteristics and engine durability [5–15]. Fuel spray studies are very important because the fuel spray directly affects the mixing of fuel with air and resulting combustion. The spray characteristics therefore directly affect the engine performance, power output and emission. However the spray characteristics are directly controlled by the physical properties of fuel therefore it is important that biodiesel spray characteristics are thoroughly investigated and their relationship with the engine performance and emission is also established well before its large scale implementation. While performing spray visualization and phase Doppler particle anemometry (PDPA) experiments, Park et al. [5] reported that biodiesel has longer spray penetration due to its

* Corresponding author. School of Mechanical Engineering, Hanyang University, 222 Wangsimni-ro, Seongdong-gu, Seoul, 04763, Republic of Korea.
E-mail address: parks@hanyang.ac.kr (S. Park).
[1] Current Affiliation: Department of Mechanical Engineering, Govt. Women Engineering College, Ajmer, 305002, India.
[2] Current Affiliation: School of Mechanical Materials and Energy Engineering, Indian Institute of Technology Ropar, Rupnagar, 140001, India.

http://dx.doi.org/10.1016/j.energy.2016.12.043
0360-5442/

Abbreviations

BMEP	Brake mean effective pressure
$BSCO_2$	Brake specific carbon dioxide
BSCO	Brake specific carbon monoxide
BSFC	Brake specific fuel consumption
BSHC	Brake specific hydrocarbon
$BSNO_X$	Brake specific oxides of nitrogen
BTE	Brake thermal efficiency
CAD	Crank angle degrees
CO_2	Carbon dioxide
CO	Carbon monoxide
CD	Combustion duration
CRDI	Common rail direct injection
CI	Compressed ignition
CAP_{max}	Crank angle position for P_{max}
$CA_{ROPRmax}$	Crank angle position for $ROPR_{max}$
CA_{10}, CA_{50}, CA_{90}	Crank angle position corresponding to different heat release percentages (10%, 50% and 90%)
DOC	Diesel oxidation catalysts
EGR	Exhaust gas recirculation
EGT	Exhaust gas temperature
FIP	Fuel injection pressure
IC	Internal combustion
KB40, KB60, KB100	40%, 60% and 100% (v/v) Karanja biodiesel blend with diesel
KOME	Karanja oil methyl ester
P_{max}	Maximum in-cylinder pressure
$ROPR_{max}$	Maximum rate of pressure rise
NO	Nitric oxide
NO_2	Nitrogen dioxide
NO_X	Oxides of nitrogen
O_2	Oxygen
PDPA	Phase Doppler particle anemometry
PM	Particulate matter
SOC	Start of combustion
SOF	Soluble organic fraction
T_{ASOE}	Time after start of energizing
THC	Total hydrocarbone
ULSD	Ultra low sulfur diesel

higher surface tension and biodiesel spray is atomized to a lesser degree in comparison to mineral diesel. Analyzing the relationships among fuel properties and engine performance, Kegl [7] concluded that higher density, viscosity and lower vapor pressure of biodiesel under high fuel injection pressure systems lead to advanced injection timings, and it also leads to earlier increase in the in-cylinder gas pressure, temperature and heat release rate compared with mineral diesel. They also reported that higher oxygen content of biodiesel results in lower smoke and carbon monoxide emissions but slightly higher hydrocarbon emissions from the engine. Various meaningful results of emission characteristics of biodiesel fuelled engines are reported in several studies [8–14]. To investigate the emission characteristics of biodiesel, especially on particulate size-number distribution in the exhaust gas, Agarwal et al. [11,12] performed engine experiment using a single cylinder research engine equipped with a common rail direct injection (CRDI) system and carried out experiments with different start of injection timings and fuel injection pressures. They reported that increasing the fuel injection pressure resulted in reduction in number concentration of particulate at all engine loads. This is because increasing fuel injection pressures led to advanced injection timings with better atomized fuel spray, and more time available for preparation of combustible mixture. Regarding trend of higher NO_X emission from biodiesel fuelled engines compared to mineral diesel, Varatharajan and Cheralathan [8] summarized several factors based on different properties of biodiesel. They suggested that advanced fuel injection timing, increased adiabatic flame temperature, higher heat release rate, and stoichiometric burning of biodiesel are possibly responsible for higher NO_X emissions from biodiesel fuelled engines. In regard to engine durability and endurance test using biodiesel, Agarwal [9] experimentally evaluated deposit formation of biodiesel on cylinder head, piston top and injector tip by performing long-term endurance test. It was reported that the carbon deposits of biodiesel fuelled engines were substantially lower than that of diesel-fuelled engine. Comparing the weight of piston deposit scrapped, it was also found that deposits in the case of biodiesel-fuelled engine were 40% lower compared to diesel-fuelled engine. In addition, carbonization level of biodiesel injector after 512 h of operation was significantly less than that of diesel injector after 200 h of engine operation.

There are various biodiesels depending on its different origin and manufacturing processes, and it is also well known that depending on their physical and chemical properties such as carbon chain length, saturation, location and types of double bond, the characteristics of engine performance and emissions would be different [10,16]. Among various types of biodiesels, Karanja oil methyl ester (KOME) is considered as one of promising biodiesels due to its non-edible origin, similar properties to diesel, as well as its easy growth characteristics even in wastelands [17].

For these reasons, several attempts were made to use Karanja biodiesel as additive with mineral diesel [18–23]. Chauhan et al. [20] investigated the performance, emissions and combustion characteristics of Karanja biodiesel blends (5%, 10%, 20%, 30% and 100%) with mineral diesel in an unmodified diesel engine. They reported 3–5% lower brake thermal efficiency with Karanja biodiesel and its blends compared to mineral diesel. It was stated that higher cetane number of biodiesel leads to shorter ignition delay, which is responsible for lower fuel accumulation in the combustion chamber during premixed combustion phase, resulting in lower heat release rate and lower peak cylinder pressure. NO_X emissions were higher while CO, smoke density and HC were reported to be lower for biodiesel compared to mineral diesel. Dhar and Agarwal [21] investigated the effect of Karanja biodiesel and its blends on engine performance, emissions and combustion characteristics in a diesel engine of a medium size utility vehicle. Slightly lower torque and higher BSFC was observed with higher blends of biodiesel. Earlier start of combustion was reported for lower biodiesel blends, while it was slightly delayed for higher biodiesel blends. Brake specific carbon monoxide (BSCO), brake specific hydrocarbon (BSHC) and smoke emissions from Karanja biodiesel blends were lower than mineral diesel but brake specific oxides of nitrogen (BSNOx) emissions were slightly higher. Barik and Sivalingam [22] conducted experiments for KOME, dual fuel KOME and biogas obtained from anaerobic digestion of Karanja de-oiled cakes in a single cylinder, four-stroke, air-cooled, diesel engine and compared the results with baseline mineral diesel. It was reported that CO, HC emissions and smoke opacity were lowest for KOME because KOME

operation was attributed to additional fuel oxygen and increased cetane number of KOME, which lowered the probability of forming a fuel rich zone and advanced the injection timings. NO_X emissions were observed to be maximum for KOME. Kaul et al. [23] characterized corrosion behavior of Karanja biodiesel by performing long duration static immersion test for 7200 h. They reported that biodiesel from Karanja oil had no significant corrosion effect on piston and liner, when compared with diesel.

Although a lot of valuable researches have been reported in open literature, there have been rather limited investigations for comprehensively understanding the relationship amongst spray characteristics, engine performance and exhaust emissions of Karanja biodiesel. Therefore the focus of this paper is to characterize the effect of blending ratio of Karanja biodiesel on spray characteristics in terms of injection rate, spray evolution process and to investigate the engine performance and emission characteristics of Karanja biodiesel blends in a CI engine compared to baseline mineral diesel.

2. Experimental setup and procedure

2.1. Spray experiment setup

Spray investigations were carried out to investigate the effect of blending ratio of Karanja biodiesel on spray behavior, spray evolution process and injection rate. The test fuels for the spray experiments were: mineral diesel as baseline (D100) fuel, 40% and 60% (v/v) blends of Karanja biodiesel (KB40, KB60), and 100% Karanja biodiesel (KB100). Depending on the blending ratio, fuel properties such as kinematic viscosity, density, and low heating value slightly differed from each other (Fig. 1). Cetane number of KB100 and mineral diesel used in this study were 50.8 and 51.2 respectively. All tests were carried out with fuel injection pressure (FIP) of 50, 100 and 150 MPa and injection duration for each FIP were calibrated for delivering injection quantity of 12 mg/pulse for all cases.

To investigate the effect of physical properties on transient needle motion of the injector and to compare maximum injection rate under different blends of biodiesel, injection rate measurement was performed. The measurement was performed using Bosch method, which measures the change in the tube pressure during fuel injection under certain back pressure and correlates it to the injection rate based on fuel quantity [24–26]. In this measurement, a back pressure of 3.0 MPa was set by referring to a previous research study about precise measurement of fuel injection rate [24]. According to their results, a back pressure higher than 2 MPa is desirable to obtain reasonable injection rate signal.

Fig. 2 shows a schematic of injection rate test bench. This bench consisted of a test injector having a hole diameter of 0.128 μm, a pressure sensor (Kistler, 4045A50), a piezo-resistive amplifier (Kistler, 4603), a data acquisition system (National Instrument, NI6013), a measuring tube 10 m in length, and a fuel drain with a relief valve for adjusting constant the back pressure.

In the measurement, fuel was injected into the measuring tube filled with fuel under a constant pressure of 3 MPa. As the fuel was injected, the pressure from the measuring tube increased, thus the pressure sensor detected increased pressure. The detected pressure signals were amplified by the piezo-resistive amplifier and were recorded by the data acquisition system. Injection quantity from the fuel drain was also measured for calculation of injection rate.

To examine and improve the accuracy of recorded injection signals, sufficient consecutive injections (over 100) were recorded. Fig. 3 shows superimposed consecutive pressure signals. These signals were ensemble averaged and represented by the red line. To ensure repeatability, each test was conducted three times and then averaged.

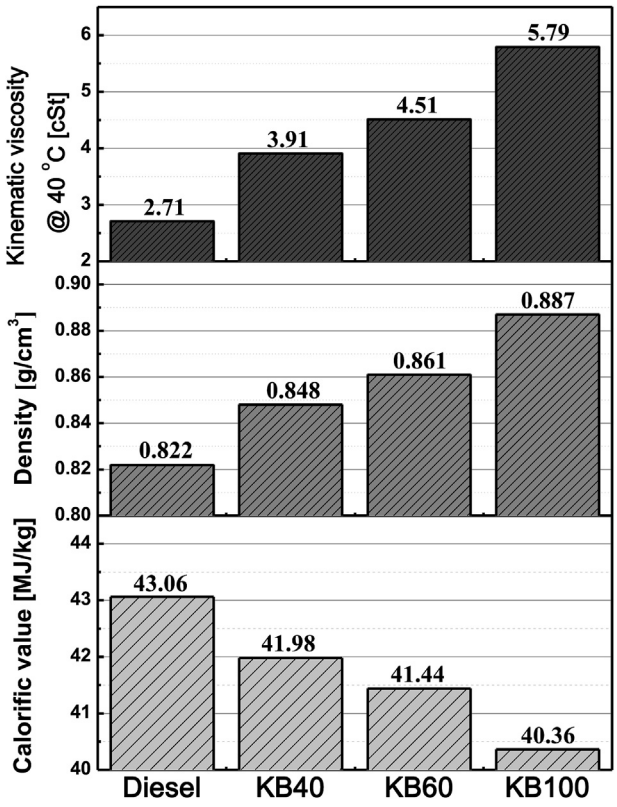

Fig. 1. Important fuel properties of test fuels.

For comparing spray evolution processes, spray visualization was performed as shown in Fig. 4. The spray visualization system mainly consisted of a constant volume spray chamber, which could be pressurize up to 6 MPa, a fuel supply system, a fuel injection system and a high-speed camera (Photron, Fastcam-APX RS). The fuel supplying system included a common-rail, a high pressure pump and a fuel tank. The fuel injection system comprised of a test injector with 6 holes, an injector driver and a digital delay/pulse generator (Berkeley Nucleonics Corp, model 575). Fuel from the fuel tank was pressurized by two high-pressure pumps working in parallel, which provided highly pressurized fuel to the test injector. The injector operating signal produced by injector driver was synchronized with the high-speed camera having a resolution of 524 × 524 pixels, equipped with 75 mm Nikon lens, using the digital delay/pulse generator, so that the images of spray were taken at the instant of 0.1 ms starting from the time after the start of energizing (T_{ASOE}). Two metal halide lamps were used as light source to illuminate the fuel spray.

To characterize the spray evolution process objectively and to quantify spray parameters such as liquid penetration, spray cone-angle, and spray boundaries for analyzing spray behavior, captured images were processed using a MATLAB based program. The fundamental procedure of image processing is illustrated in Fig. 5. The captured images were converted into binary images for separation of spray from the background. After separation with fixed threshold of 10% for the instantaneous luminosity, boundary pixels were calculated to quantify spray parameters such as spray penetration and spray cone angle. The spray penetration is defined as the distance from the nozzle tip to the maximum outer point of each spray and the spray cone angle is defined as the angle of nozzle tip generated by the two intersecting lines from the two outer regions of each spray for widest distance between them at a

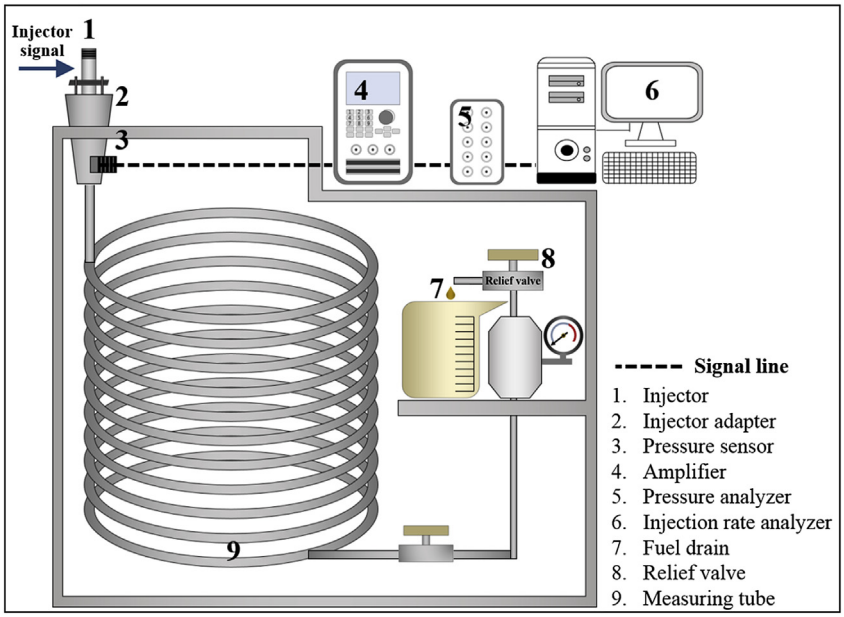

Fig. 2. Schematic of fuel injection rate measurement.

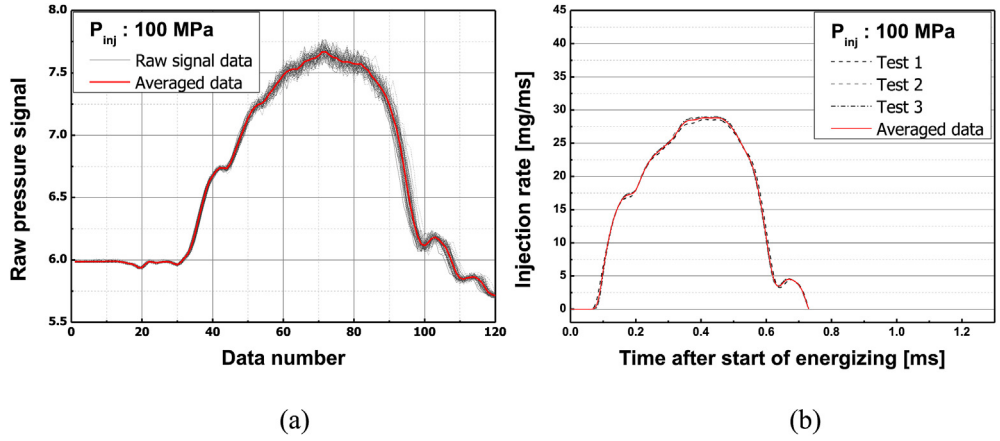

Fig. 3. Raw pressure signal data and average process (a) superimposed consecutive pressure signals (b) ensemble averaged signal.

distance of 70%, penetration length.

2.2. Engine experiment setup

Schematic of the engine experimental setup is shown in Fig. 6. A four cylinder, water cooled, CRDI 2.2 L, Euro IV SUV (Safari DICOR, Tata Motors India) diesel engine was used for the experimental investigations. Technical details for the experimental engine are provided in Table 1.

This test engine was enabled with turbocharger (variable geometry), intercooler and after-treatment technology such as exhaust gas recirculation (EGR) and two diesel oxidation catalysts (DOC). Tests were performed on CRDI engine fuelled with KB40 and mineral diesel as baseline fuel. Consequently, engine performance, combustion and emissions characteristics were compared for both fuels. For engine performance characteristics, a laminar flow meter (Cussons: P7205/150) and a volumetric flow meter was used for air and fuel consumption rates respectively.

Engine exhaust emissions were sampled and measured for various regulated gaseous emissions using a raw exhaust gas emission analyser (Horiba; EXSA-1500). Raw exhaust gas emission analyser measured the concentration of carbon monoxide (CO), carbon dioxide (CO_2), total hydrocarbon (THC), oxides of nitrogen (NO_X), and oxygen (O_2) with high accuracy. Raw exhaust gas emission analyser included CO/CO_2 analyser (NDIR detector: MCA-220UA), HC analyser (Hot flame ionization detector: FIA-225UA) and NO_X analyser (Chemiluminescence detector: CLA-220UA).

Measuring ranges [27] of the raw exhaust gas emission analyser are given in Table 2. For comparison across different engine test point, raw emission data from the exhaust gas emission analyser was converted to the mass emissions i.e. brake specific emissions using IS: 14273 code [28]. The exhaust opacity was measured using smoke opacimeter (AVL; 437). A piezoelectric pressure transducer (AVL; GH13P) and a charge amplifier (Kistler; 5015A00X0) were used for in-cylinder pressure measurement for combustion analysis. Cylinder pressure signals and crank-shaft rotation were synchronized using a high precision crank-angle incremental optical shaft encoder (BEI: XH25D-SS-3600-ABZC-28V/V-SM18, Resolution: 10 pulses per CAD), which was installed on the engine crankshaft. For acquisition and analysis of cylinder pressure-crank angle data, a

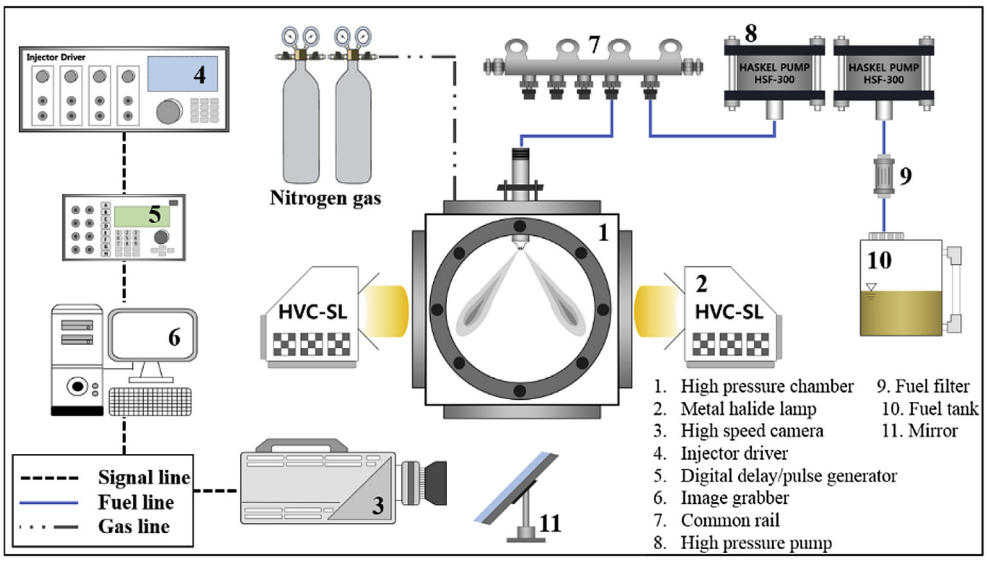

Fig. 4. Schematic of spray visualization experiment.

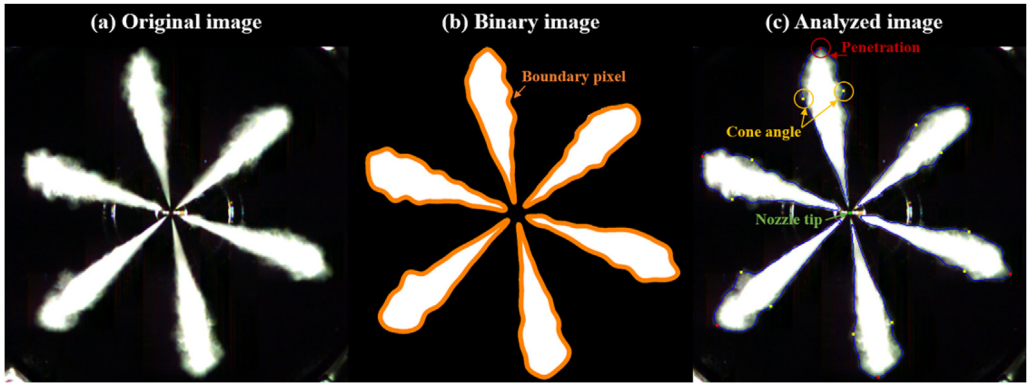

Fig. 5. Image processing procedures (a) original image (b) binary image (c) analyzed image.

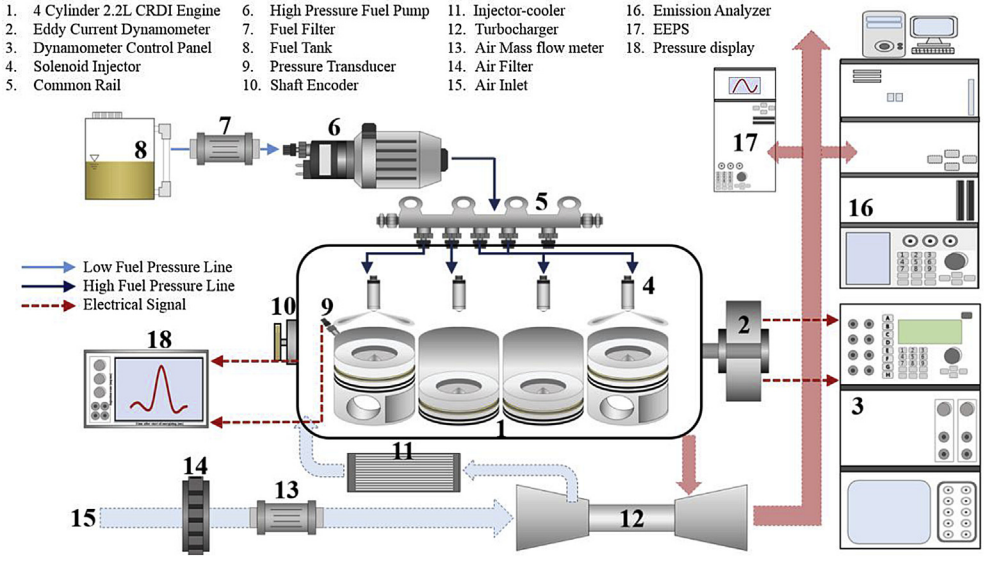

Fig. 6. Schematic of the engine experimental setup.

Table 1
Technical specifications of the test engine.

Make/Model	Tata/Dicor 2.2L (BS-IV/Euro-IV)
Engine Type	16 valves, Water cooled, CRDI, Turbocharged, and Intercooled Diesel Engine with Exhaust gas recirculation system.
No. of cylinder	4, In-line
Valve Mechanism	DOHC
Bore/Stroke	85 mm × 96 mm
Cubic Capacity	2179 cc
Max. Engine Output	103 kW @ 4000 rpm
Maximum Torque	320 Nm @ 1700–2700 rpm
Compression ratio	17.5
Firing order	1-3-4-2
FIE System	CRDI with 1600 bar max fuel injection pressure
Fuel filter	Single stage fuel filter
Fuel Injection Pump	High Pressure Pump

high speed combustion data acquisition system (Hi-Techniques: Synergy) was used. Engine exhaust particle sizer (EEPS) spectrometer (TSI; 3090) was used for particle number and size distribution of the test engine for both test fuels. EEPS measures particle sizes ranging from 5.6 to 560 nm with a size resolution of 16 channels per decade (a total of 32 channels) upto a maximum concentration of 10^8 particles/cm^3 in the engine exhaust using a rotating disk thermo-diluter (Matter Engineering; MD19-2E).

2.3. Engine experiment procedure

Based on the detail comparison of spray evolution processes using Karanja biodiesel blends, engine experiments for analyzing combustion and emission characteristics were conducted for KB40 and baseline mineral diesel under similar test conditions. Performance characteristics (speed-torque curve, BSFC, BTE, EGT), emissions analysis (CO_2, CO, NO_X, HC, Smoke opacity), combustion analysis (In-cylinder pressure, rate of heat release, cumulative heat release, combustion duration) and Particle size distribution were characterized for KB40 and mineral diesel at no load, 20%, 40%, 60%, 80% and 100% for rated engine speed of 2500 rpm. These results for performance, combustion and emissions were also compared for same fuels at 100% load at 1500, 2000, 2500, 3000 and 3500 rpm engine speeds. Variations in cylinder pressure with crank angle was recorded for 200 consecutive engine cycles and then averaged in order to eliminate the effect of cycle-to-cycle variations. This averaged cylinder pressure data was used to calculate heat release rate, mass-burn fraction crank angles, combustion duration and other combustion related parameters. Number concentration of the exhaust particulates was measured in the diluted exhaust and concentrations in the engine exhaust was calculated by accounting for the dilution factor.

3. Results and discussion

3.1. Injection rate characteristics

Fig. 7 shows the results of injection rates for different FIP of 50, 100 and 150 MPa in a constant ambient pressure of 3 MPa. At 50 MPa FIP, slightly higher injection rate of diesel with faster opening and closing of needle were observed compared with Karanja biodiesel blends. As increased FIP (i.e., 150 MPa), biodiesel blends showed higher injection rate than baseline mineral diesel and this difference was magnified with increasing blending ratio of biodiesel in the test fuel. These results suggested that the transient needle motion and the maximum injection rate were strongly influenced by the fuel properties such as viscosity and density. Relatively higher viscosity of biodiesel resulted in slower needle movement at fuel injection pressure of 50 MPa. However, with increasing FIP, the effect of viscosity reduced due to increased fuel flow rate, and higher fuel density of biodiesel blends led to increased maximum fuel injection rates. Similar results were also reported by Desantes et al. [29] and Moon et al. [30].

Table 2
Measuring ranges of raw exhaust gas emission analyser [27].

Species	Measurement Principle	Measurement Range
CO	NDIR	0-5000 ppm
CO_2	NDIR	0-10/20% (v/v)
NO_X	Chemiluminescence	0-100/500/1000/5000 ppm
THC	FID	100/500/1000/5000/10000/50000 ppm C
O_2	Magnetic Pressure	0-10/25% (v/v)

3.2. Spray evolution process

Fig. 8 represents the boundary pixels of the spray showing spray evolution at FIP of 50, 100 and 150 MPa in the ambient pressure of 2 and 4 MPa. The boundary imaging data was used to analyze spray evolution and the influence of blending ratio on spray penetration, and spray cone angle. For all FIPs, the injected fuel quantity was kept constant at 12 mg/pulse. It is evident from Fig. 8 that increasing FIP led to faster evolution of spray, thus the elapsed time to reach the given distances (e.g., 20 mm and 30 mm) reduced. The ambient pressure also has a strong influence on the spray behavior, thus increasing ambient pressure results in wide distribution of fuel spray and longer time to reach a given distance. Based on comparison of spray evolution of mineral diesel and biodiesel blends, faster spray evolution of diesel can be observed at 50 MPa, especially for the penetration of 30 mm. This can be thought to the effect of high viscosity of Karanja biodiesel, which is consistent with the results of injection rate. Thus the delayed needle opening led to retarded spray evolution process for biodiesel blends. However with increasing FIP, longer spray penetration was measured for biodiesel and blends, and this trend magnified with increasing blends of biodiesel. For 4 MPa ambient pressure, quite similar spray evolutions were observed. Higher blends of Karanja biodiesel showed increased spray penetration however the difference reduced compared to 2 MPa ambient pressure primarily due to higher resistance from the ambient air. Overall spray evolution of KB40 was similar to that of mineral diesel for its spray penetration and cone angle at any given elapsed time.

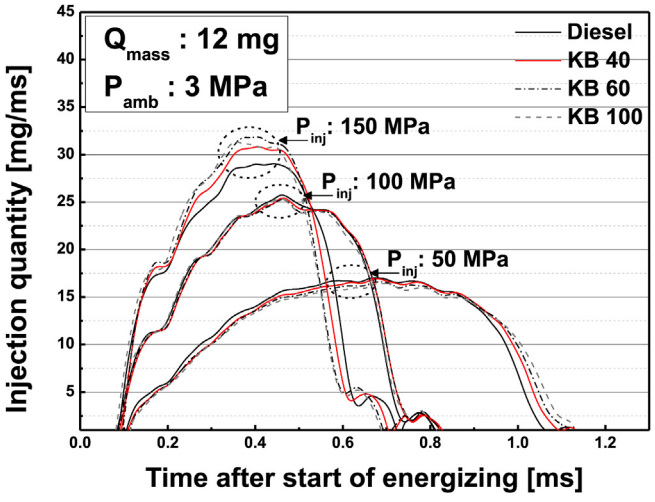

Fig. 7. Comparison of injection rate for various injection pressure, P_{inj}: 50, 100 and 150 MPa, P_{amb}: 3 MPa.

For better comparison of spray characteristics to the engine experiments, overall spray evolution from KB40 and diesel were compared under the ambient pressures of 4 MPa, which is considered to be similar to the in-cylinder pressure of test engine at the end of compression stroke. Fig. 9 shows spray evolution for mineral diesel and KB40 under FIPs of 50, 100, 150 MPa. As shown in Fig. 9, the initial spray evolution of KB40's spray was slightly faster than that of baseline diesel. The spray shape of KB40 also showed narrower spray cones and deeper penetrating evolution of the spray aligned to its axis. This observation suggests that the injection of KB40 was more advanced and its relatively faster response could be due to higher density of Karanja biodiesel.

Fig. 10 shows a comparison of spray cone angle of diesel and KB40 under different injection pressures. To represent reliable comparison of spray cone angle, the cone angle of each of the plumes were averaged. The spray cone angles of diesel were wider under ambient pressure of 2 MPa, especially in the initial stages of spray evolution before the T_{ASOE} of 0.8 ms. These differences in spray cone angles were found to reduce with increasing ambient pressure up to 4 MPa. These results showed the influence of different physical properties of KB40 on spray evolution, which reduces significantly under ambient pressure of 4 MPa. Thus KB40 can be thought to behave almost similar as that of mineral diesel and therefore can be used in an engine without any hardware modifications or adjustments.

3.3. Engine performance

Based on the spray experiments and some references reporting experimental results about engine combustion, exhaust emission fuelled with biodiesel-diesel blends [31,32], it emerges that Karanja biodiesel can be used in diesel engines without any modification in injectors. Thus, engine test were performed for KB40 and diesel in the present study.

Fig. 11 compares the speed-torque characteristics of KB40 and mineral diesel. Maximum torque achieved for speeds between 2000 and 2500 rpm for both fuels was found to be slightly lower for KB40 compared to mineral diesel and at higher speed of 3000 rpm; KB40 delivered slightly higher torque than mineral diesel. However the difference in torque between diesel and KB40 was statistically insignificant.

Fig. 12 (a) and (b) show the relationship between engine performance characteristics such as brake thermal efficiency (BTE), brake specific fuel consumption (BSFC) and exhaust gas temperature (EGT) versus brake mean effective pressure (BMEP) and engine speed respectively for KB40 and baseline diesel.

BTE and EGT showed increasing trend with increasing load for both test fuels. BTE was observed to be relatively lower for biodiesel blends at all test conditions compared to baseline diesel. At the same time, BSFC was observed to be relatively higher for KB40 compared to baseline diesel for all test conditions. Since BSFC was calculated on mass basis, higher density of biodiesel resulted in higher BSFC. These trends are also obvious since engine consumes more fuel quantity for same power output, owing to relatively lower calorific value of Karanja biodiesel compared to diesel. Similar results for higher BSFC were also obtained by other researchers for Mahua and Karanja biodiesels [33–35]. EGT increased with engine load from 170 °C at no load to 650 °C at full load at 2500 rpm. This is because of more fuel consumed to cater to higher engine loads. EGT was observed to be slightly lower for KB40 compared to diesel at the same load and speed combinations. This can be possibly an effect of biodiesel combustion being longer compared to diesel and its shorter ignition delay [36].

Brake specific carbon monoxide (BSCO), brake specific carbon dioxide ($BSCO_2$), brake specific oxides of nitrogen ($BSNO_X$) emissions vs. BMEP and engine speed are shown in Fig. 13. For consistency, these emissions are shown in mass emissions (g/kW-h or kg/kW-h).

BSCO emission decreased with increasing engine loads for both test fuels. Since with increased load, air intake quantity also increases, leading to more complete combustion of fuel, it leads to reduced BSCO emissions. Slight differences in CO emissions were observed for both test fuels at all test conditions. $BSCO_2$ emissions decreased with increasing engine loads while they increased with increasing engine speeds. $BSCO_2$ emissions were observed to be relatively lower for KB40, compared to diesel, possibly due to

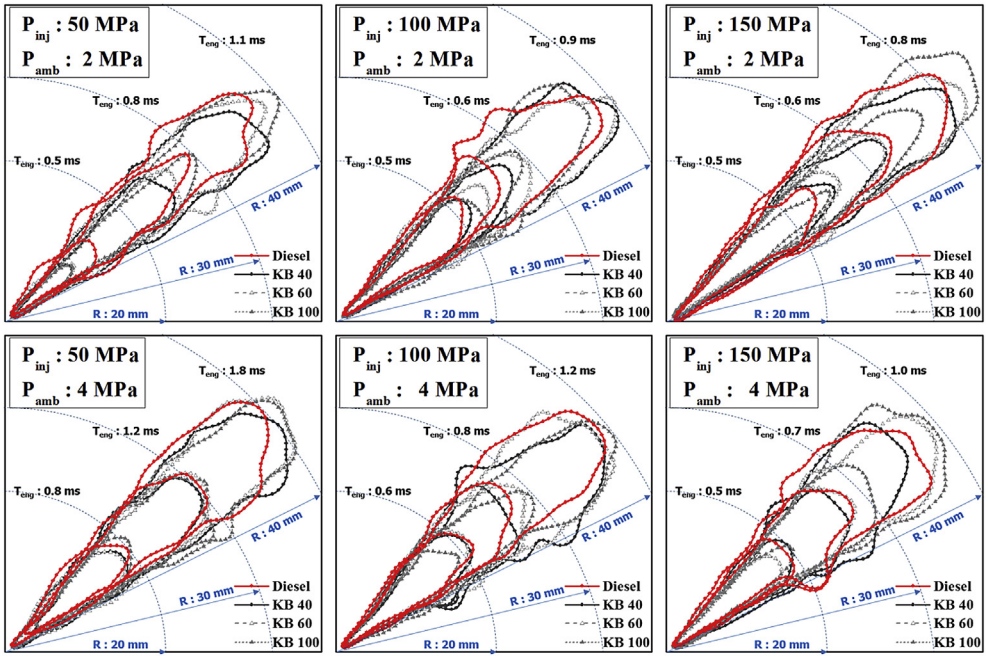

Fig. 8. Comparison of spray evolution process, P_{inj}: 50, 100 and 150 MPa, P_{amb}: 2 and 4 MPa.

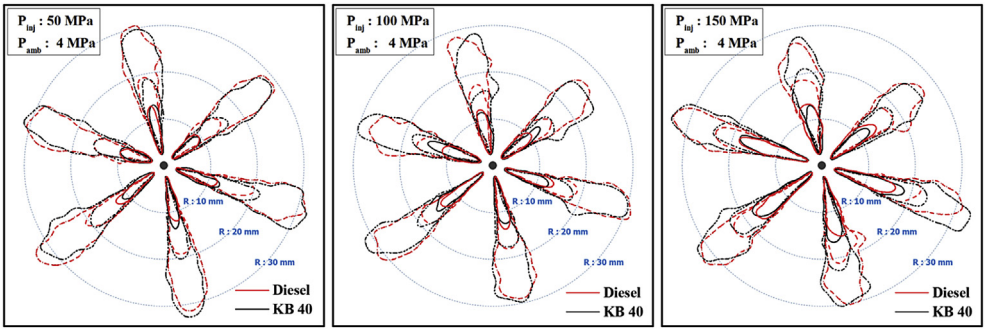

Fig. 9. Comparison of spray evolution of KB40 and mineral diesel, P_{inj}: 50, 100 and 150 MPa, P_{amb}: 4 MPa.

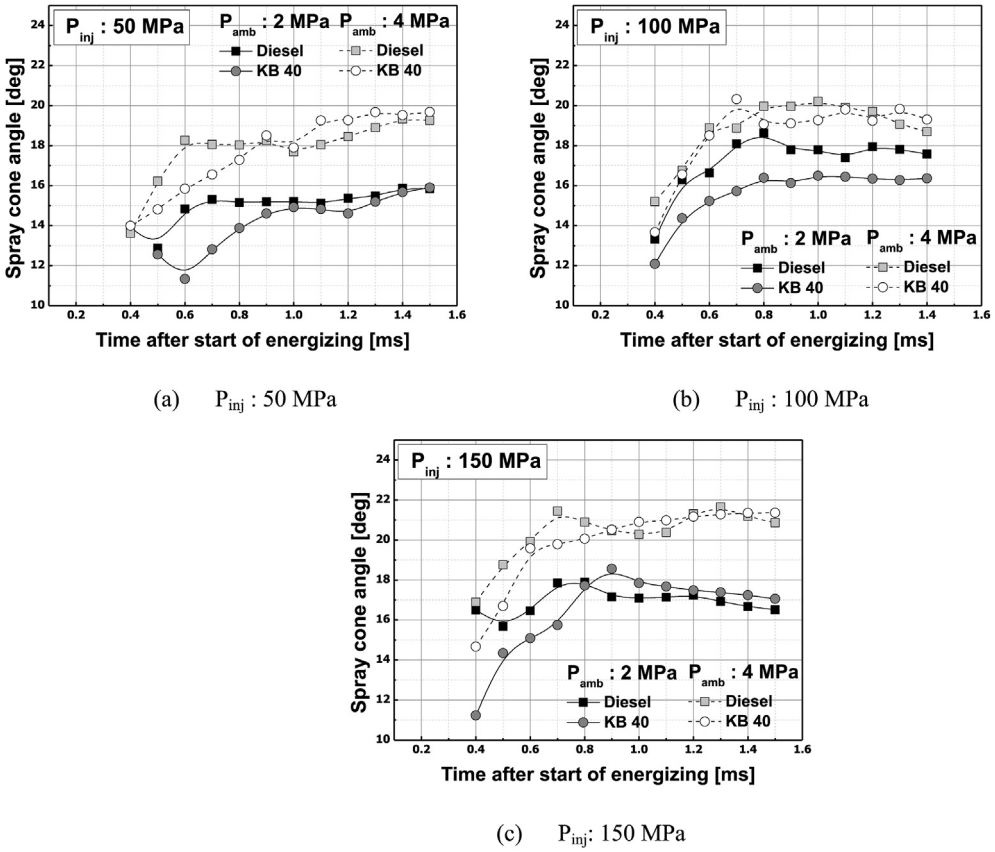

Fig. 10. Comparison of spray cone angle of KB40 and diesel, P_{inj}: 50, 100 and 150 MPa, P_{amb}: 2 and 4 MPa.

additional inherent oxygen available in the biodiesel fuel molecule. Oxides of nitrogen emissions comprise of mainly nitrogen oxide (NO) and nitrogen dioxide (NO_2), where NO is the predominant species formed inside the combustion chamber. NO_X emissions were found to be relatively higher for KB40 at most operating conditions. This was possibly due to higher combustion temperatures due to improved combustion because of inherent oxygen in biodiesel. Relatively earlier start of combustion was primarily due to advanced injection timings caused by relatively higher bulk modulus and higher density of Karanja biodiesel. Under some conditions, NO_X emissions from KB40 were nearly same as that of baseline diesel. This may be attributed to relatively lower calorific value and higher cetane number of Karanja biodiesel, which causes reduced heat release rate during premixed combustion thereby relatively lower peak combustion temperatures [37]. NO_X level was observed to be directly related to the peak in-cylinder temperature, while it is inversely related to the smoke opacity and CO emission [33].

Variations in BSHC and smoke opacity with BMEP and engine speed were also compared for KB40 and diesel as shown in Fig. 14.

There was no particular relationship observed for BSHC emissions for the test fuels. Fuel bound oxygen improved combustion and reduced HC emissions. Higher HC formation for KB40 may be due to locally over-rich fuel-air mixture. Similar results were also reported by Chandan Kumar et al. [38]. They showed higher unburnt hydrocarbon emissions at lower load and vice versa for Karanja biodiesel compared to diesel. Smoke opacity reduced significantly with biodiesel addition to mineral diesel for all operating conditions, which was primarily due to oxygen enrichment of the test fuel. Addition of oxygenates in the fuel leads to improved diffusive combustion, when smoke is produced. Smoke opacity increased with increasing engine load, which was due to reduced

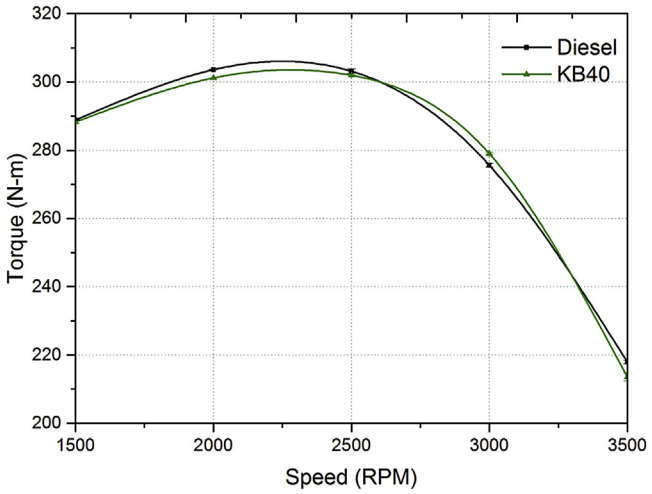

Fig. 11. Speed-Torque characteristics curve.

air-fuel ratio at higher engine load. At such conditions, higher fuel quantity is injected into the combustion chamber, where part of this fuel goes out unburnt, thus increasing the smoke opacity.

Particulate matter (PM) comprises of dry carbon particles (soot), soluble organic fraction (SOF) and traces of sulfates and nitrates. Fig. 15 shows particle number concentration vs. particle size at 2500 rpm engine speed with load variations from no load to rated load.

Nucleation mode particles (below 50 nm) were observed to be higher for KB40 compared to diesel at almost all test conditions. Tan et al. [39] suggested three main causes for this trend. First, higher viscosity and lower volatility of biodiesel could lead to slower evaporation and air-fuel mixing inside the combustion chamber [40], which causes increased SOF formation, thereby contributing to nucleation mode particle formation. Second, reduced accumulation mode particles cause reduced solid soot surfaces thereby reduced SOF adsorption and condensation on soot particles, whereas high super-saturation may lead to increased nucleation particles. Third, oxygenated fuel causes carbonaceous particles changing from fine sizes to ultrafine sizes or even nano-particles, resulting in increased numbers of nucleation mode particles. Ye et al. [41] conducted experiments using ultra-low sulfur diesel (ULSD) and B40 blend of soybean methyl ester with ULSD in a turbocharged CRDI diesel engine and concluded that biodiesel fuelling has more significant effect on PM emissions at lower loads and a less significant effect at moderate to high loads. Song et al. [42] concluded that relatively higher rate of oxidation of biodiesel origin soot particles compared to mineral diesel origin soot particles, primarily due to surface oxygen functionality of fuel-bound oxygen in biodiesel, may be the main reason for reduced particle size distribution and higher numbers of smaller nano-particles.

Fig. 16 shows total PM number concentration vs. engine load at 2500 rpm for both test fuels. Fig. 17 illustrates total particulate number concentration vs. engine speed at rated load. Total particulate number accounts for both, nucleation and accumulation mode particles. Higher total particulate number concentration was observed for KB40 compared to diesel at all test conditions. At higher loads (80–100%), significantly higher total particulate number concentrations were observed, due to domination of nucleation mode particles.

Fig. 18 shows the comparison of in-cylinder pressure, rate of heat release and cumulative heat release for diesel, and KB40 at 2500 rpm for (a) 0% (b) 60% (c) 100% rated load.

It can be observed from Fig. 18 that KB40 has slightly higher peak in-cylinder pressure compared to diesel at almost all loads. Relatively higher peak in-cylinder pressure for KB40 was observed possibly due to higher cetane number and oxygen content of biodiesel, which led to shorter ignition delay during combustion. Also shorter ignition delay causes lower peak heat release rate due to

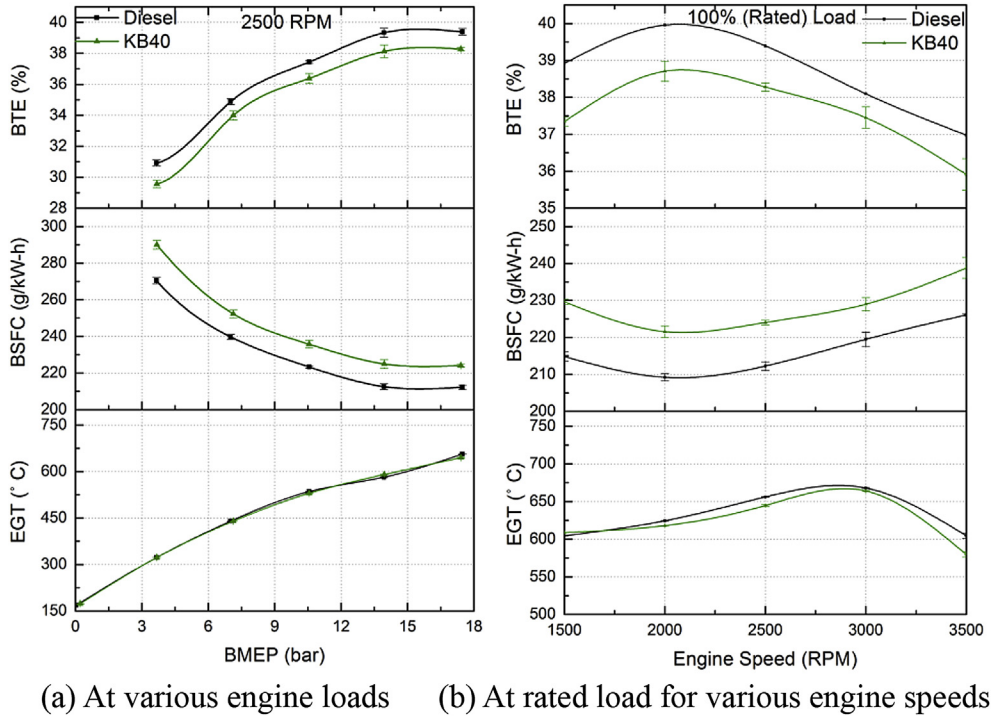

Fig. 12. Brake thermal efficiency, Brake specific fuel consumption and Exhaust gas temperature for diesel and KB40.

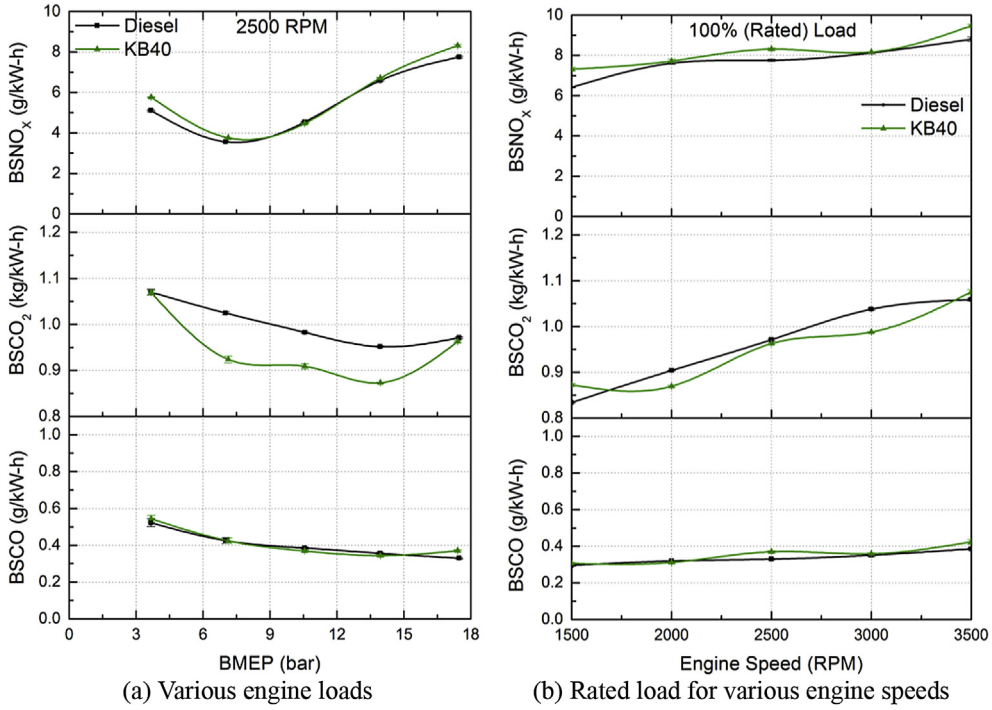

Fig. 13. Brake specific Carbon monoxide (BSCO), Brake specific Carbon dioxide ($BSCO_2$), brake specific oxides of Nitrogen ($BSNO_X$) emissions with load.

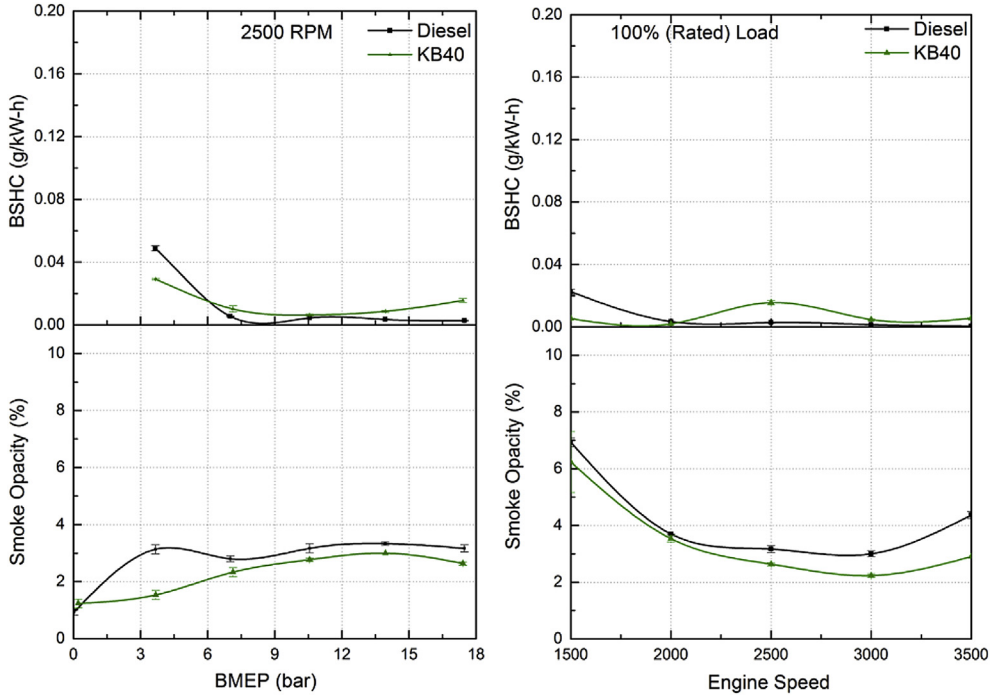

Fig. 14. Brake specific hydrocarbon emission and Smoke opacity with (a) BMEP and (b) engine speed.

lower amount of fuel accumulated in the premixed heat release period.

Fig. 19 shows the variation of maximum in-cylinder pressure (P_{max}), crank angle position of P_{max} (CA_{Pmax}), maximum rate of pressure rise ($ROPR_{max}$) and crank angle position of $ROPR_{max}$ ($CA_{ROPRmax}$) with varying engine load for diesel and KB40 at 2500 rpm engine speed.

Fig. 19 shows that maximum in-cylinder pressure increased with increasing engine load for both test fuels. Maximum in-cylinder pressure for KB40 was slightly higher compared to diesel. For lower load (40% Load), maximum in-cylinder pressure occurs close to TDC for both test fuels. Reason for this behavior of the engine was programming of ECU at low loads. Engine ECU automatically select the number of pilot injections and their

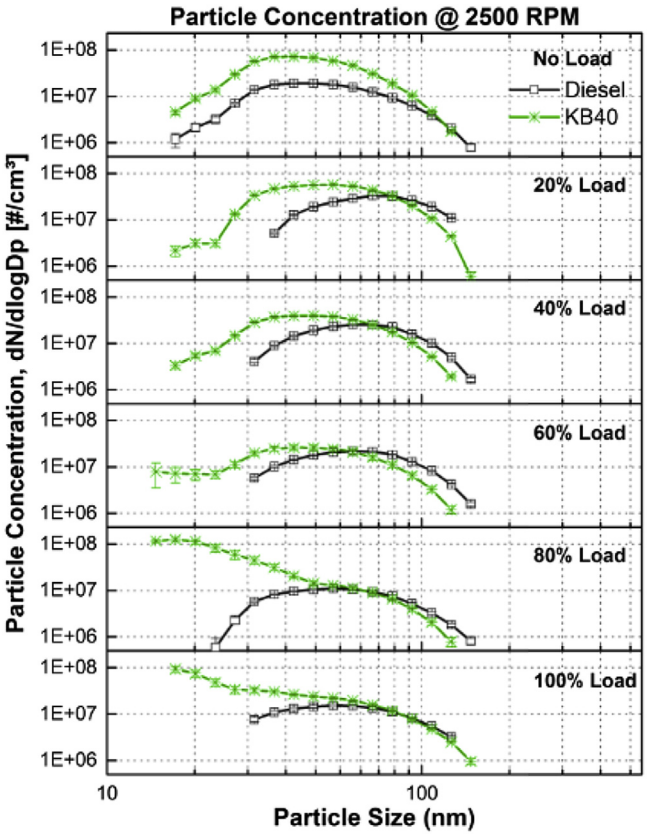

Fig. 15. Particle size number distribution with varying engine load.

position based on engine map generated by engine manufacture. To control the pressure rise rate, number of pilot injections and their position was automatically decided by ECU. It can be observed from Fig. 18 (a) and (b) that for 0% and 60% engine load case have two local maxima points in cylinder pressure graphs. Based on the quantity of pilot injection, any of those can have higher values. Therefore 40% and 60% engine load have CA_{Pmax} values close to TDC. For higher loads, CA_{Pmax} was away from the TDC and in all test conditions; CA_{Pmax} was lower than 15 CAD after top dead center

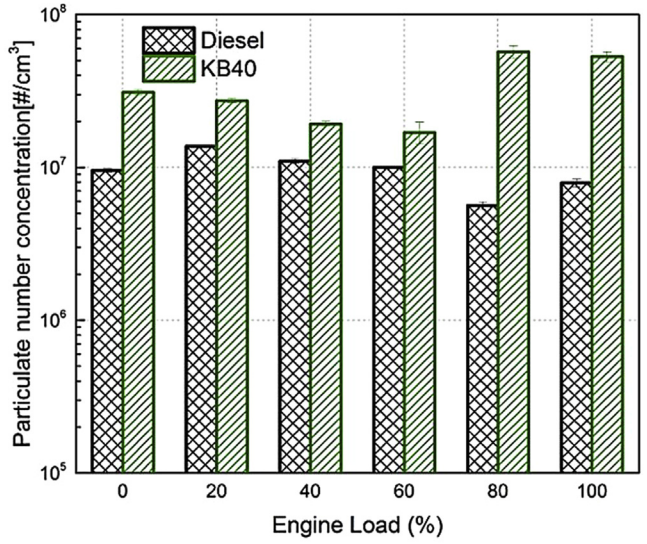

Fig. 16. Particulate number concentration vs. engine load.

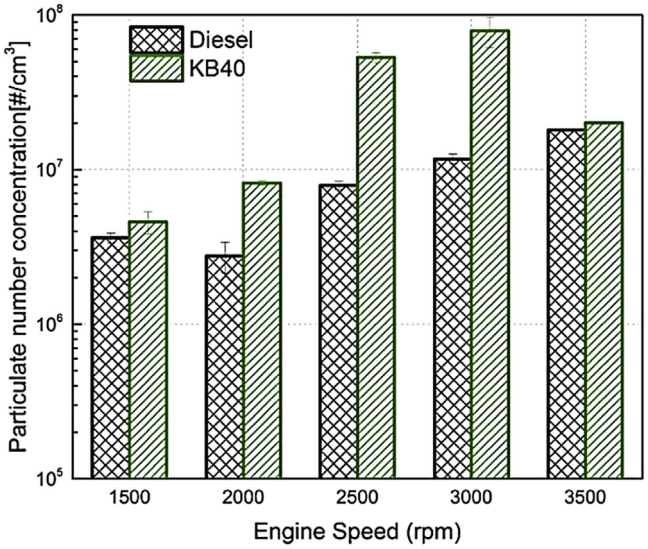

Fig. 17. Particulate number concentration at rated load vs. engine speed.

(aTDC). At higher engine loads, single peak pressure was observed in cylinder pressure curve therefore it shows CA_{Pmax} away from TDC position.

Maximum ROPR is an indicator of harshness of combustion. From Fig. 19, it was observed that $ROPR_{max}$ was less than 6 bar/CAD for both test fuels. It can also be noticed that $ROPR_{max}$ increased with increasing engine load. KB40 showed higher $ROPR_{max}$ for most test conditions compared to diesel, which showed relatively noisy combustion for KB40. Scholl et al. [43] also reported similar results that P_{max} and $ROPR_{max}$ was higher for SME than diesel. Sahoo et al. [44] also showed higher P_{max} and lower ignition delay for Polanga, Jatropha and Kanranja biodiesel compared to diesel in their experiments. Crank angle position corresponding to $ROPR_{max}$ was before TDC upto 80% load for both test fuels, which suggests that $ROPR_{max}$ corresponds to the pilot injection. However, $CA_{ROPRmax}$ was after TDC at full load, possibly corresponding to the main injection. At full load engine operation, main fuel injection quantity was comparatively larger than pilot injection quantity, therefore pressure raise rate was possibly more due to main injection and it appeared after TDC position.

Rate of heat release (RoHR) was calculated using high speed combustion data acquisition system based on measured in-cylinder pressure data. Crank angle position corresponding to different heat release percentages (10%, 50% and 90%) in the engine cylinder were calculated and represented as CA_{10}, CA_{50} and CA_{90} respectively. Crank angle position corresponding to 10% heat release (CA_{10}) was used as an indication of start of combustion (SOC) in this investigation. Difference of crank angle position between 90% and 10% heat release is defined as 'combustion duration' for this study.

Fig. 20 shows the variation of crank angle position corresponding to CA_{10}, CA_{50}, CA_{90} and combustion duration (CD) with engine load for diesel and KB40 at 2500 rpm engine speed.

At higher engine loads, SOC was relatively advanced for diesel compared to KB40. CA_{50} was found to be in the range of 5–15° CA for both test fuels. At higher loads, CA_{50} position was identical for both test fuels at tested engine speed. It can also be observed from Fig. 20 that combustion process ends late for biodiesel blend compared to diesel at 2500 rpm. For most test conditions, CA_{90} position was less than 36° CA aTDC. Similar results for late end of combustion for rice-bran oil biodiesel blend compared to diesel were reported by Sinha et al. [45]. They suggested that faster RoHR for diesel as well as lower volatility and higher flash point of

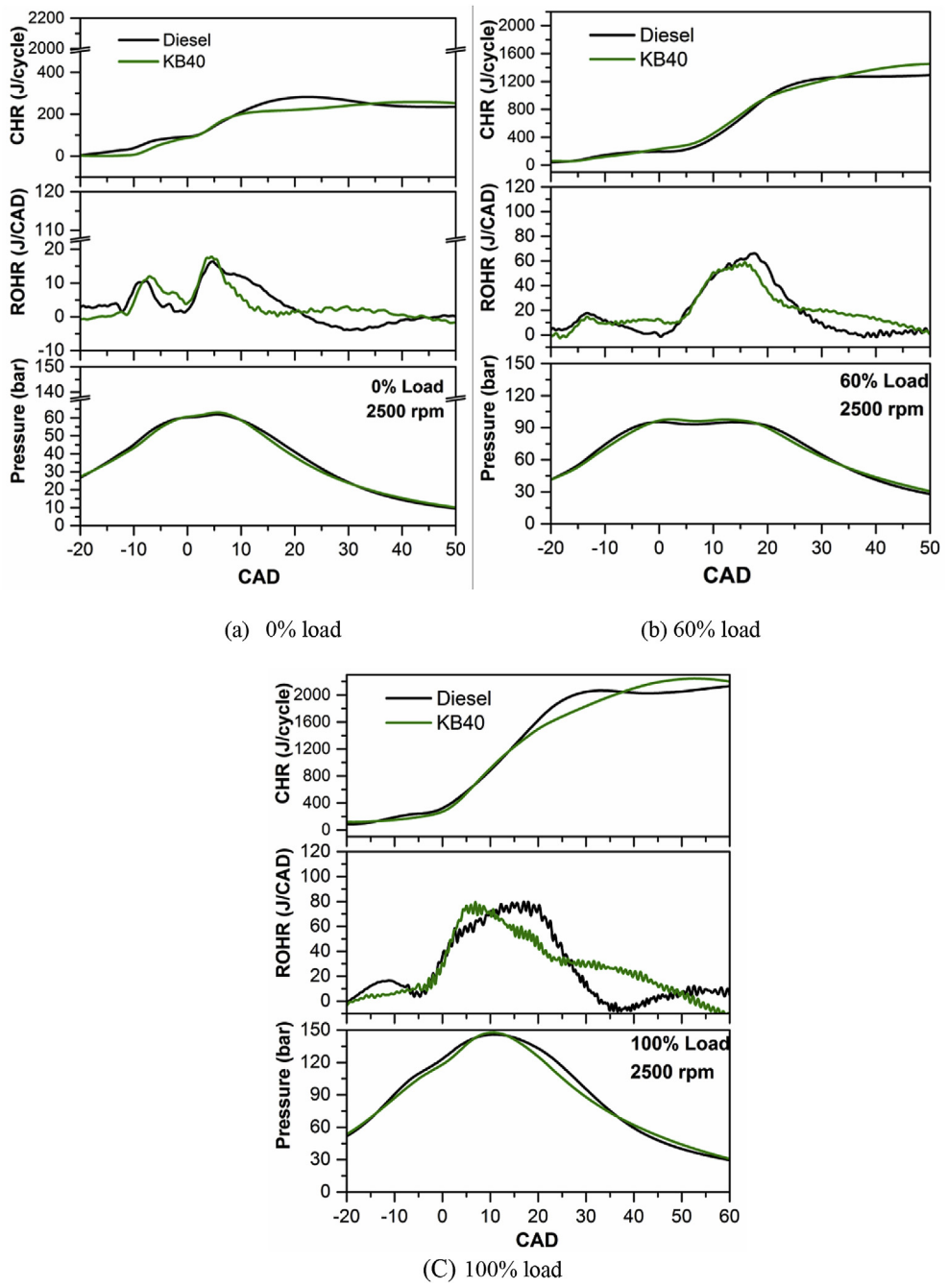

Fig. 18. Comparison of in-cylinder pressure, rate of heat release and cumulative heat release for diesel and KB40 at 2500 rpm.

biodiesel (183 °C) caused relatively slower burning of biodiesel.

Fig. 20 also shows combustion duration for KB40 and diesel at 2500 rpm engine speed. KB40 has longer combustion duration compared to diesel at tested engine speed of 2500 rpm. Combustion duration for all test conditions was in range 25–50° CA. Combustion duration first increased with increasing engine load and then towards the full load condition, it started decreasing. Quantity of injected fuel also increased with increasing engine load, which tends to increase the time required for completion of combustion. Also more fuel is required in case of KB40 because of its relatively lower calorific value compared to diesel, which led to longer combustion duration for biodiesel [45]. With increasing engine load, in-cylinder temperature also increased, which increased the rate of air-fuel mixing as well as rate of evaporation. Resultant effect of these two opposing factors led to longest combustion duration at intermediate engine loads for both test fuels. Pradeep and Sharma [46] also concluded higher combustion duration and lower RoHR for rubber seed oil biodiesel and blends in a single cylinder diesel engine compared to baseline diesel.

4. Conclusions

The purpose of this study was to understand the effect of Karanja biodiesel blending on fuel spray characteristics and to correlate it with the engine performance and emissions characteristics by comparing with baseline diesel. This paper demonstrated the

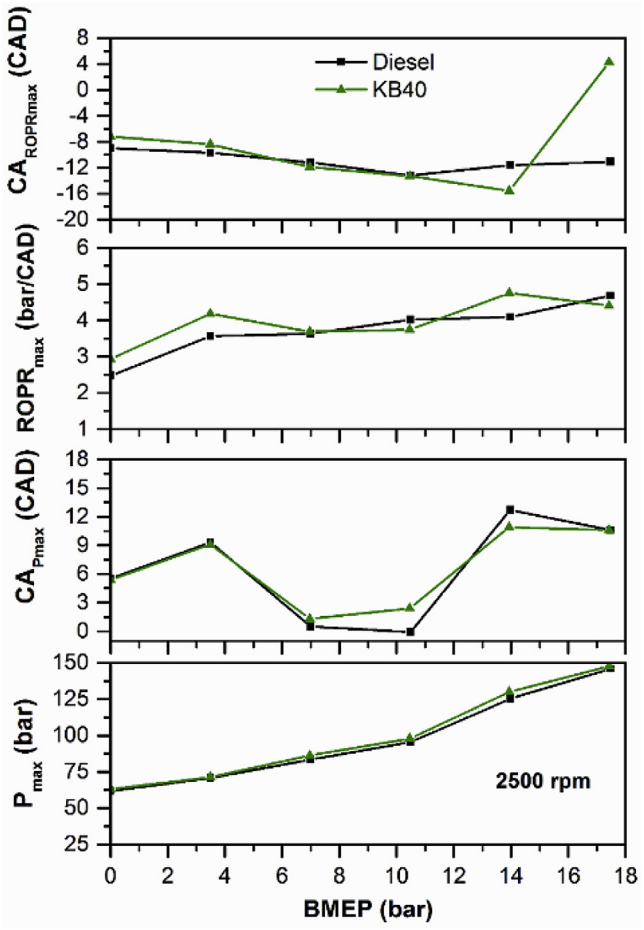

Fig. 19. Variation of maximum in-cylinder pressure (P_{max}), crank angle position of P_{max} (CA_{Pmax}), maximum rate of pressure rise ($ROPR_{max}$) and crank angle position of $ROPR_{max}$ ($CA_{ROPRmax}$) with varying engine load.

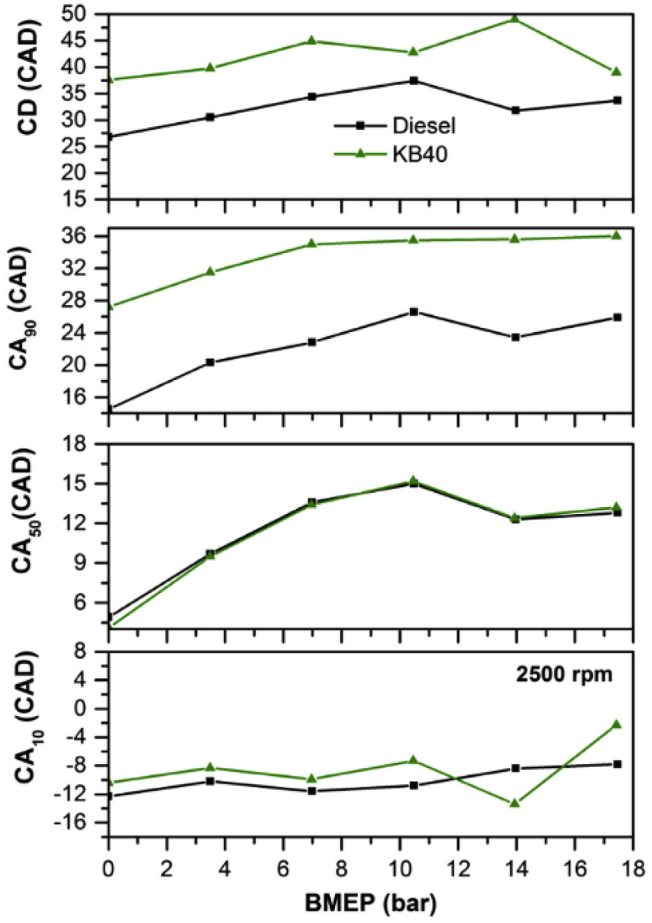

Fig. 20. Crank angle position corresponding to 10% (CA_{10}), 50% (CA_{50}), 90% (CA_{90}) mass burn fraction and combustion duration (CD) vs. engine load.

spray evolution process and injection rate in relation to engine performance and emissions for KB40 and diesel. The main findings of this study are as follows:

1. At the fuel injection pressure of 50 MPa, slightly higher injection rate of diesel compared with Karanja biodiesel blends was observed because of faster opening and closing of the needle. However, as the fuel injection pressure increased (up to 150 MPa), biodiesel blends showed higher injection rate compared to mineral diesel and this difference was seen in the curve of maximum injection rate. Thus difference increased with increasing blending ratio of biodiesel.

2. Relatively faster spray evolution of diesel compared to biodiesel blends can be observed for FIP of 50 MPa, especially under the spray penetration depth of 30 mm. This can be thought as the effect of relatively higher viscosity of Karanja biodiesel. The trends are consistent with the results of injection rate, thus the delayed needle opening led to retarded spray evolution of biodiesel blends. However, for higher FIPs, longer penetration was observed for biodiesel and blends. This trend was also magnified with increasing blending ratio of biodiesel.

3. At an ambient pressure of 2 MPa, the initial penetration of KB40 spray was slightly shorter compared to that of diesel. The spray shape of KB40 spray also showed relatively narrower and deeper penetrating spray evolution. However for higher ambient pressure of 4 MPa, KB40 showed a quite similar spray evolution process for diesel in terms of spray penetration and spray shape. The influence of different physical properties of KB40 on spray development can be neglected under higher ambient pressure of 4 MPa.

4. Lower maximum torque, BTE and EGT but higher BSFC were observed for biodiesel blends compared to baseline diesel because of lower calorific value of Karanja biodiesel. In addition, lower $BSCO_2$, and higher NO_X emissions were observed for KB40, possibly due to inherent fuel oxygen present in biodiesel molecules. BSHC and BSCO emissions were found to be very low for both test fuels.

5. Smoke opacity of KB40 was lower than baseline diesel for most experimental conditions. However, higher number concentration of total particulate and nucleation mode particles below 50 nm were observed for KB40 compared to baseline diesel because of higher viscosity and lower volatility of biodiesel.

6. At higher engine loads, SOC was relatively advanced for baseline diesel compared to KB40. KB40 showed relatively longer combustion duration compared to mineral diesel at tested engine speed of 2500 rpm. Combustion duration for test conditions was between 25 and 50° CA.

References

[1] Shahir VK, Jawahar CP, Suresh PR. Comparative study of diesel and biodiesel on CI engine with emphasis to emissions—a review. Renew Sustain Energy Rev 2015;45:686–97.
[2] Naik M, Meher LC, Naik SN, Das LM. Production of biodiesel from high free fatty acid Karanja (Pongamia pinnata) oil. Biomass Bioenergy 2008;32:354–7.
[3] Yoon SH, Park SH, Lee CS. Experimental investigation on the fuel properties of biodiesel and its blends at various temperatures. Energy & Fuels 2007;22:

652–6.
[4] Zhang J, Jing W, Roberts WL, Fang T. Effects of ambient oxygen concentration on biodiesel and diesel spray combustion under simulated engine conditions. Energy 2013;57:722–32.
[5] Park SH, Cha J, Kim HJ, Lee CS. Effect of early injection strategy on spray atomization and emission reduction characteristics in bioethanol blended diesel fueled engine. Energy 2012;39:375–87.
[6] Mohan B, Yang W, Tay KL, Yu W. Experimental study of spray characteristics of biodiesel derived from waste cooking oil. Energy Convers Manag 2014;88:622–32.
[7] Kegl B. Influence of biodiesel on engine combustion and emission characteristics. Appl Energy 2011;88:1803–12.
[8] Varatharajan K, Cheralathan M. Influence of fuel properties and composition on NOx emissions from biodiesel powered diesel engines: a review. Renew Sustain Energy Rev 2012;16:3702–10.
[9] Agarwal AK. Biofuels (alcohols and biodiesel) applications as fuels for internal combustion engines. Prog Energy Combust Sci 2007;33:233–71.
[10] Pullen J, Saeed K. Factors affecting biodiesel engine performance and exhaust emissions – Part I: Review. Energy 2014;72:1–16.
[11] Pullen J, Saeed K. Factors affecting biodiesel engine performance and exhaust emissions – Part II: experimental study. Energy 2014;72:17–34.
[12] Agarwal AK, Gupta T, Shukla PC, Dhar A. Particulate emissions from biodiesel fuelled CI engines. Energy Convers Manag 2015;94:311–30.
[13] Agarwal AK, Dhar A, Gupta JG, Kim WI, Lee CS, Park S. Effect of fuel injection pressure and injection timing on spray characteristics and particulate size–number distribution in a biodiesel fuelled common rail direct injection diesel engine. Appl Energy 2014;130:212–21.
[14] Banapurmath NR, Tewari PG, Hosmath RS. Experimental investigations of a four-stroke single cylinder direct injection diesel engine operated on dual fuel mode with producer gas as inducted fuel and Honge oil and its methyl ester (HOME) as injected fuels. Renew Energy 2008;33:2007–18.
[15] Hwang J, Qi D, Jung Y, Bae C. Effect of injection parameters on the combustion and emission characteristics in a common-rail direct injection diesel engine fueled with waste cooking oil biodiesel. Renew Energy 2014;63:9–17.
[16] Kumar N, Varun, Chauhan SR. Performance and emission characteristics of biodiesel from different origins: a review. Renew Sustain Energy Rev 2013;21:633–58.
[17] Takase M, Zhao T, Zhang M, Chen Y, Liu H, Yang L, et al. An expatiate review of neem, jatropha, rubber and karanja as multipurpose non-edible biodiesel resources and comparison of their fuel, engine and emission properties. Renew Sustain Energy Rev 2015;43:495–520.
[18] Lingfa P, Krishnan Unni J, Naik SN, Das LM. A comparative study on performance and emission characteristics of compression ignition engine using biodiesel derived from non-edible feedstocks. SAE Pap 2013-01-2676. http://dx.doi.org/10.4271/2013-01-2676
[19] Pandey AK, Sivakumar P, Nandgaonkar M, Suresh S. Comparison and evaluation of engine wear, combustion and emissions performance between diesel, karanja and jatropha oil methyl ester biodiesel in a 780 hp military diesel engine. SAE Pap 2014-01-1395. http://dx.doi.org/10.4271/2014-01-1395
[20] Chauhan BS, Kumar N, Cho HM, Lim HC. A study on the performance and emission of a diesel engine fueled with Karanja biodiesel and its blends. Energy 2013;56:1–7.
[21] Dhar A, Agarwal AK. Performance, emissions and combustion characteristics of Karanja biodiesel in a transportation engine. Fuel 2014;119:70–80.
[22] Barik D, Sivalingam M. Investigation on performance and exhaust emissions characteristics of a DI diesel engine fueled with karanja methyl ester and biogas in dual fuel mode. SAE Pap 2014-01-1311. http://dx.doi.org/10.4271/2014-01-1311.
[23] Kaul S, Saxena RC, Kumar A, Negi MS, Bhatnagar AK, Goyal HB, et al. Corrosion behavior of biodiesel from seed oils of Indian origin on diesel engine parts. Fuel Process Technol 2007;88:303–7.
[24] Takamura A, Ohta T, Fukushima S, Kamimoto T. A study on precise measurement of diesel fuel injection rate. SAE paper 920630.
[25] Bower GR, Foster DE. A comparison of the Bosch and Zuech rate of injection meters. SAE paper 910724.
[26] Arcoumanis C, Baniasad MS. Analysis of consecutive fuel injection rate signals obtained by the Zeuch and Bosch methods. SAE paper 930921.
[27] Operational and Instruction Manual, MEXA-1500 exhaust gas analyzer, Horiba Ltd., Japan.
[28] Indian standard IS: 14273. Automotive vehicles – exhaust emissions – gaseous pollutants from vehicles fitted with compression ignition engines – method of measurement. New Delhi, India: Bureau of Indian Standards; 1999.
[29] Desantes JM, Payri R, García A, Manin J. Experimental study of biodiesel blends' effects on diesel injection processes. Energy & Fuels 2009;23:3227–35.
[30] Moon S, Tsujimura T, Gao Y, Park S, Wang J, Kurimoto N, et al. Biodiesel effects on transient needle motion and near-exit flow characteristics of a high-pressure diesel injector. Int J Engine Res 2013. 1468087413497951.
[31] Gumus M, Sayin C, Canakci M. The impact of fuel injection pressure on the exhaust emissions of a direct injection diesel engine fueled with biodiesel–diesel fuel blends. Fuel 2012;95:486–94.
[32] Sayin C, Gumus M, Canakci M. Effect of fuel injection pressure on the injection, combustion and performance characteristics of a DI diesel engine fueled with canola oil methyl esters-diesel fuel blends. Biomass Bioenergy 2012;46:435–46.
[33] Raheman H, Ghadge SV. Performance of compression ignition engine with mahua (Madhuca indica) biodiesel. Fuel 2007;86:2568–73.
[34] Raheman H, Phadatare AG. Diesel engine emissions and performance from blends of karanja methyl ester and diesel. Biomass Bioenergy 2004;27:393–7.
[35] Kousoulidou M, Fontaras G, Ntziachristos L, Samaras Z. Biodiesel blend effects on common-rail diesel combustion and emissions. Fuel 2010;89:3442–9.
[36] Canakci M. Combustion characteristics of a turbocharged DI compression ignition engine fueled with petroleum diesel fuels and biodiesel. Bioresour Technol 2007;98:1167–75.
[37] Teoh YH, Masjuki HH, Kalam MA, Amalina MA, How HG. Impact of waste cooking oil biodiesel on performance, exhaust emission and combustion characteristics in a light-duty diesel engine. SAE Pap 2013-01-2679. http://dx.doi.org/10.4271/2013-01-2679.
[38] Kumar C, Gajendra Babu MK, Das LM. Experimental investigations on a karanja oil methyl ester fueled DI diesel engine. SAE Pap 2006-01-0238. http://dx.doi.org/10.4271/2006-01-0238.
[39] Tan P-q, Hu Z-y, Lou D-m, Li B. Particle Number and Size Distribution from a Diesel Engine with Jatropha Biodiesel Fuel. SAE paper 2009-01-2726.
[40] Yamane K, Ueta A, Shimamoto Y. Influence of physical and chemical properties of biodiesel fuels on injection, combustin and exhaust emission characteristics in a direct injection compression ignition engine. Int J Engine Res 2001;2:249–61.
[41] Ye P, Boehman AL. An investigation of the impact of injection strategy and biodiesel on engine NOx and particulate matter emissions with a common-rail turbocharged DI diesel engine. Fuel 2012;97:476–88.
[42] Song J, Alam M, Boehman AL. Impact of alternative fuels on soot properties and DPF regeneration. Combust Sci Technol 2007;179:1991–2037.
[43] Scholl KW, Sorenson SC. Combustion of soybean oil methyl ester in a direct injection diesel engine. SAE paper 930934.
[44] Sahoo PK, Das LM. Combustion analysis of Jatropha, Karanja and Polanga based biodiesel as fuel in a diesel engine. Fuel 2009;88:994–9.
[45] Sinha S, Agarwal A. Experimental investigation of the combustion characteristics of a biodiesel (rice-bran oil methyl ester)-fuelled direct-injection transportation diesel engine. Proc Institution Mech Eng Part D J Automob Eng 2007;221:921–32.
[46] Pradeep V, Sharma RP, Evaluation of performance, emission and combustion parameters of a CI engine fuelled with bio-diesel from rubber seed oil and its blends, SAE Pap 2005-26-353. http://dx.doi.org/10.4271/2005-26-353